2014

Kondorski reversal in magnetic nanowires

Ralph A. Skomski
University of Nebraska-Lincoln, rskomski2@unl.edu

Eva Schubert
University of Nebraska-Lincoln, efranke3@unl.edu

Axel Enders
University of Nebraska-Lincoln, a.enders@me.com

David J. Sellmyer
University of Nebraska at Lincoln, dsellmyer@unl.edu

Kondorski reversal in magnetic nanowires

Ralph Skomski,[1,a)] Eva Schubert,[2] Axel Enders,[1] and D. J. Sellmyer[1]
[1]*Department of Physics and Astronomy, Nebraska Center for Materials and Nanoscience, University of Nebraska, Lincoln, Nebraska 68588, USA*
[2]*Department of Electrical Engineering, University of Nebraska, Lincoln, Nebraska 68588, USA*

(Presented 5 November 2013; received 25 September 2013; accepted 13 November 2013; published online 5 March 2014)

Magnetization reversal in nanowire systems, such as alnico-type permanent magnets, slanted columns produced by glancing-angle deposition, and nanowires embedded in alumina templates, is investigated by model calculations. The angular dependence of the domain-wall propagation is Kondorski-like, reminiscent of Kondorski pinning in bulk materials but with a somewhat different physics and consistent with Kerr hysteresis-loop measurements. Criss-cross patterning of alnicos improves the coercivity but reduces the remanence, with virtually zero net effect on energy product. Finally, we briefly discuss the wire-radius dependence of the coercivity in the context of "shape anisotropy" and the occurrence of interaction domains in alnico. © *2014 AIP Publishing LLC*. [http://dx.doi.org/10.1063/1.4865975]

I. INTRODUCTION

Soft-magnetic or semihard wires with diameters of the order of 100 nm are an important class of magnetic nanostructures, serving as nanoscale building blocks for various applications. Examples are alnico permanent magnets,[1–3] wires deposited electrochemically into alumina templates,[4–7] and slanted nanowires (columns) fabricated by glancing-angle deposition (GLAD).[8] For example, alnico permanent magnets consist of elongated soft-magnetic regions of FeCo embedded in a nonmagnetic NiAl matrix. Simplifying somewhat, the magnetic FeCo and nonmagnetic NiAl phases separate by spinodal decomposition and crystallize in cubic bcc derivatives such as the cubic B2 (CsCl) and, depending on additives, $L2_1$ (Heusler). Alnicos, which underwent a rapid development between 1932 and 1966,[2] continue to be used industrially and have attracted renewed interest due to threatened rare-earth supplies. Furthermore, there are several poorly understood features, for example, the role of elemental additives such as Cu, Ti, and Nb.[9] From a technological viewpoint, the limiting factor is coercivity: each percent in coercivity increase or decrease counts, so that relatively small anisotropy changes (such as 10% due to interface anisotropy) have a pronounced industrial effect. The main origin of coercivity of alnicos is shape anisotropy,[1,2,10] although this terms needs careful consideration (Sec. III) and interface anisotropy is not necessarily negligible.[11] Our emphasis is on the angular dependence of the coercivity, which is described in form of a modified Kondorski model.

The original Kondorski model[12] dates back to the 1930s and is basically the earliest coercivity model, developed for bulk materials and antedating the Stoner-Wohlfarth model.[13] Figure 1(a) shows the basic idea. The domain wall motion during magnetization reversal is driven by the Zeeman energy proportional to $\mathbf{M}\cdot\mathbf{H}$, so that only the projection of the field onto the magnetization contributes. For Bloch walls in bulk magnets, this yields $H_c = H_o/\cos\theta$, Fig. 1(b), where H_o is the coercivity if M and H are parallel. H_o depends on the real structure of the magnet, as described by the domain wall energy $\gamma(x)$.

II. KONDORSKI MECHANISM IN NANOWIRES

The elongated shape of the magnetic columns and the smallness of the magnetocrystalline anisotropy mean that the magnetization prefers to remain parallel to the columns (or

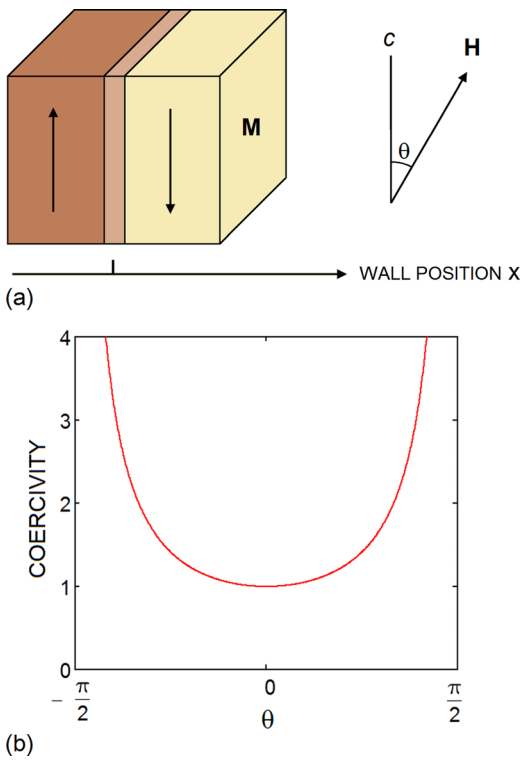

FIG. 1. Kondorski mechanism in bulk magnets: (a) schematic picture and (b) angular dependence of the normalized coercivity $H(\theta)/H_o$.

[a)]Author to whom correspondence should be addressed. Electronic mail: rskomski@neb.rr.com.

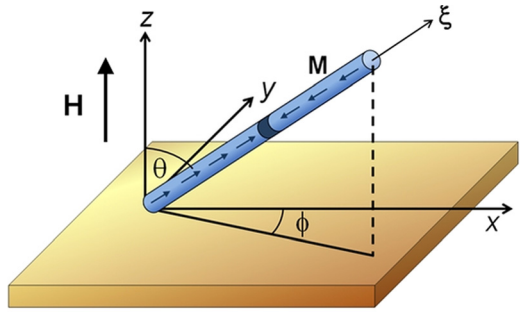

FIG. 2. Nanowire geometry and orientation.

needles or wires). As a consequence, magnetization reversal proceeds by domain-wall motion, as contrasted to coherent rotation. Figure 2 shows the geometry for arbitrary wire orientations. As in the bulk case, the domain-wall motion is driven by the field component parallel to $\pm\mathbf{M}$, that is, parallel to the wires.

Denoting the domain-wall position by ξ and the domain-wall energy by $\gamma(\xi)$, we obtain

$$E_{\text{wall}}(\xi) = \pi R^2\gamma(\xi) - 2\pi R^2\mu_o M_s H_p \xi. \tag{1}$$

Here, $H_p = p$, where H is the field component parallel to the wire, p is the projection cosine of the angle between field and magnetization, and R is the cross-section radius of the wire. The equilibrium condition $dE(\xi)/d\xi = 0$ yields the pinning field

$$H_c = \frac{\max|d\gamma/d\xi|}{2p\,\mu_0 M_s} \tag{2}$$

or $H_c = H_o/p$.

In the GLAD geometry, with $\phi \neq 0$ and an in-plane field $\mathbf{H} = H_x\,\mathbf{e}_x$, the direction cosine $p = \cos\phi\,\sin\theta$ connects the x- and ξ-axes, so that

$$H_c(\phi) = \frac{H_0}{\cos\phi\,\sin\theta}. \tag{3}$$

To probe the angular dependence of the magnetic hysteresis, we have used GLAD to deposit permalloy (Py) nanowires and determined the coercivity from hysteresis-loop measured by vector magneto-optical generalized ellispsometry (Vector-MOGE, see, e.g., Ref. 8). In the nanowires, the angle $\theta \approx 65°$ is fixed by the deposition process, and the x-axis can be chosen so that $\phi = 0$. Comparing the coercivities for fields in the x and z directions, we obtain $H_o/\cos(90°–65°)$ and $H_o/\cos(65°)$, respectively (Table I). The means that a field rotation from the x-axis to the z-axis

TABLE I. Coercivity values from the magnetic hysteresis loops of slanted Py nanowires measured with variable external fields in the x- and z-directions and nanowire orientation in the x-z plane.

Magnetic field orientation	$H = H_0\,e_x$	$H = H_0\,e_z$
Coercivity (T)	0.065	0.137

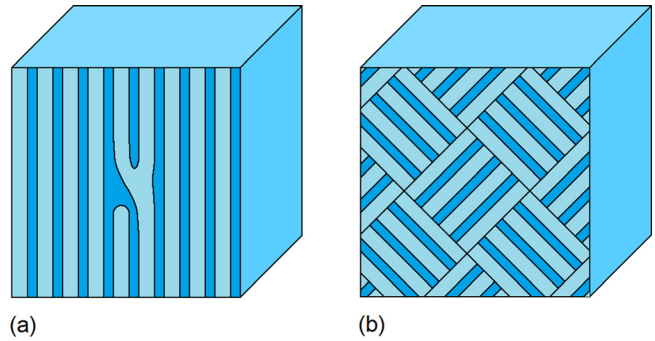

FIG. 3. Alnico microstructures (schematic): (a) anisotropic alnico and (b) criss-cross patterned alnico. Figure 1(a) is typical of Alnico 8–9 industrial magnets.[2]

enhances the theoretical coercivity by a factor of $\cos(25°)/\cos(65°) = 2.14$. The respective experimental values, obtained from Kerr hysteresis loops, are 0.137 T and 0.065 T, which yields a ratio of 2.11.

III. ANGULAR EFFECTS IN ALNICOS

In anisotropic alnicos, the growth direction of the Fe-Co needles can be tuned via the angle of the applied magnetic field.[9] Figure 3 shows typical microstructures. In (b), the Fe-Co needles grow along the ⟨001⟩ direction that has the largest projection onto the field.

How do the oblique angles affect coercivity and energy product? Application of Eq. (4), with $\phi = 0$ and $\mathbf{H} = H_z\,\mathbf{e}_z$, yields $H_c \sim 1/\cos\theta$, the same expression as for the bulk Kondorski model but with a different physical meaning. On the other hand, the remanence M_r is proportional to the magnetization projection onto the field direction, that is, to $M_r \sim \cos\theta$. For small coercivities, as in the case of alnico, the energy product $(BH)_{max}$ scales as $M_r\,H_c$ and is in lowest order independent of the angle θ. This means that criss-cross patterning can be used to tune H_c vs. M_r, creating magnetic design flexibility, but the energy product remains largely unchanged during the tuning.

IV. DOMAIN-WALL NUCLEATION

Even if the magnetization reversal proceeds by domain wall motion and the coercivity is determined by pinning, the reversal starts by the *nucleation* of a domain wall at the nucleation field H_N, normally starting from the wire ends. The corresponding angular dependence is generally more complicated than for the Kondorski mechanism (see, e.g., p. 188 in Ref. 6).

An important aspect of nucleation in alnico magnets is the dependence on the radius R of the wires, because the spinodal decomposition process prevents R from becoming very small. It has been known since the 1940s that flux-closure, curling, or "vortex-likes" spin configurations affect the nucleation field. The analysis was first made for spherical particles[14] but also applies to elongated particles.[15] Figure 4 compares this curling mode (b) with the coherent-rotation or Stoner-Wohlfarth mode (a). The corresponding equations are well-known, and explicitly comparing the corresponding

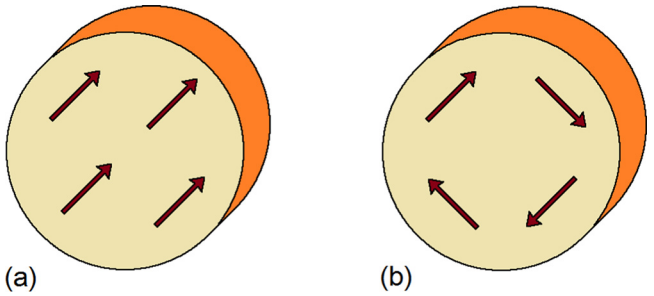

FIG. 4. Nucleation mechanisms in thin wires: (a) coherent rotation and (b) curling. Both types of nucleation typically start at wire ends and then lead to domain-wall propagation.

nucleation fields[16] for very long ellipsoids (needles) yields the Stoner-Wohlfarth nucleation field

$$H_N = \frac{1}{2}M_s. \tag{4}$$

This expression is limited to very thin wires, that is, to very small diameters $2R$. For large diameters, this shape anisotropy is destroyed by internal flux closure, Fig. 4(b), and the corresponding curling nucleation field is

$$H_N = \frac{6.678A}{\mu_o M_s R^2}, \tag{5}$$

where A is the exchange stiffness. In this practically relevant regime, the nucleation field increases with the exchange (A) and decreases with the magnetization (M_s), so that the traditional term "shape anisotropy" is somewhat unfortunate.

As a function of wire radius, the nucleation field is constant ($M_s/2$) for thin wires ($R < R_{coh}$) and decreases as $1/R^2$ for thick wires ($R < R_{coh}$) where the coherence radius[16] $R_{coh} = 3.655\ (A/\mu_o M_s^2)^{1/2}$, or approximately $R_{coh} = 6.4$ nm for $Fe_{63}Co_{35}$. This trend has been verified experimentally, in electrodeposited nanowires.[5] Note that the FeCo needles are typically much thicker than $2R_{coh} = 12.8$ nm, which is one reason for the low coercivity of alnicos.

V. INTERACTION DOMAINS

Another interesting aspect of alnicos is the occurrence of interaction domains. Figure 3(a) indicates that the magnetic needles in alnico are not always separated but occasionally touch each other. This creates exchange bridges between wires, which affect the micromagnetism of the alnicos.

Without exchange-bridges, the predominant interaction between the wires is antiparallel or "antiferromagnetic" via magnetic pole at the ends of the needles. However, the bridges create a parallel or "ferromagnetic" coupling between wires, and the coupling energy is equal to the energy of the domain walls in the bridges. The corresponding domain-wall energy cannot be estimated from the usual expression $\gamma = 4(AK_1)^{1/2}$, because the anisotropy constant K_1 is approximately zero for soft magnets. In fact, the domain-wall energy is determined magnetostatically, by the pole distribution near the wall, and approximately equal to $\mu_o M_s^2 R^3$. On the other hand, the competing magnetostatic interactions between the poles at the wire ends yield an energy contribution scaling as $\mu_o M_s^2 R^3 (R/D)$, where D is the center-to-center distance. This means the parallel coupling via the exchange bridges wins the competition, though not by a big margin, and enable the formation of ground-state interaction domains via the percolation of exchange bridges.

VI. CONCLUSIONS

In summary, we have investigated magnetization processes in soft-magnetic thin wires, with emphasis on permalloy needles produced by GLAD and alnico magnets. The angular dependence of the domain-wall propagation in the wires is governed by a modified Kondorski law, and our Kerr-effect coercivity measurements on the permalloy nanowires confirm these predictions. In alnicos, the angular dependence can be used to change coercivity and remanence, but this tuning leaves the energy product nearly unchanged.

ACKNOWLEDGMENTS

This research was supported by DOE (BREM), NSF-MRSEC (DMR-0820521), and NCMN. Thanks a due to Bill McCallum, Lin Zhou, Matt Kramer, Steve Constantinides, and Malcolm Stocks for stimulating discussions related to alnico.

[1]F. E. Luborsky, L. I. Mendelsohn, and T. O. Paine, J. Appl. Phys. **28**, 344 (1957).
[2]R. A. McCurrie, *Ferromagnetic Materials—Structure and Properties* (Academic Press, London, 1994).
[3]R. Skomski and J. M. D. Coey, *Permanent Magnetism* (Institute of Physics, Bristol, 1999).
[4]D. J. Sellmyer, M. Zheng, and R. Skomski, J. Phys.: Condens. Matter **13**, R433 (2001).
[5]H. Zeng, R. Skomski, L. Menon, Y. Liu, S. Bandyopadhyay, and D. J. Sellmyer, Phys. Rev. B **65**, 134426 (2002).
[6]R. Skomski, H. Zeng, M. Zheng, and D. J. Sellmyer, Phys. Rev. B **62**, 3900 (2000).
[7]M. Zheng, R. Skomski, Y. Liu, and D. J. Sellmyer, J. Phys.: Condens. Matter **12**, L497 (2000).
[8]D. Schmidt, C. Briley, E. Schubert, and M. Schubert, Appl. Phys. Lett. **102**, 123109 (2013).
[9]Q. Xing, M.-K. Miller, L. Zhou, H.-M. Dillon, R. W. McCallum, I. E. Anderson, S. Constantinides, and M. J. Kramer, IEEE Trans. Magn. **49**(7), 3314 (2013).
[10]R. Skomski, Y. Liu, J. E. Shield, G. C. Hadjipanayis, and D. J. Sellmyer, J. Appl. Phys. **107**, 09A739 (2010).
[11]R. Skomski, P. Manchanda, P. Kumar, B. Balamurugan, A. Kashyap, and D. J. Sellmyer, IEEE Trans. Magn. **49**(7), 3215 (2013).
[12]E. J. Kondorski, Phys. Z. Sowjetunion **11**, 597 (1937).
[13]E. C. Stoner and E. P. Wohlfarth, Philos. Trans. R. Soc. London, Ser. A **240**, 599 (1948).
[14]W. F. Brown, *Micromagnetics* (Wiley, New York, 1963).
[15]A. Aharoni, *Introduction to the Theory of Ferromagnetism* (University Press, Oxford, 1996).
[16]R. Skomski, J. Phys.: Condens. Matter **15**, R841 (2003).